

Supporting Information

Phosphor-Converted Warm White Laser Diodes with High Saturation Threshold Through PiGF-Dual Sapphire Converter

Hongjin Zhang^a, Mingxi Liang^a, Han Chen^a, Jiuzhou Zhao^a, Ning Li^b, Ziliang Hao^b,
Mingxiang Chen^c, Xiaowei Liu^{*a}, and Yang Peng^{*a}

- a) School of Aerospace Engineering, Huazhong University of Science and Technology,
Wuhan 430074, China.
E-mail: liuxiaowei@hust.edu.cn, ypeng@hust.edu.cn
- b) Wuhan Raycus Fiber Laser Technologies Company, Wuhan 430000, China
- c) School of Mechanical Science and Engineering, Huazhong University of Science and
Technology, Wuhan 430074, China

Thermal simulation

The heat power was calculated by the difference between laser power and light power of R-PiGF-D ($P_{\text{heat}} = P_{\text{laser}} - P_{\text{light}}$), ($P_{\text{laser}}=8 \text{ W/mm}^2$). A deposited beam power which

consistent with the Gaussian distribution is applied on the PiGF

$(f(o,e) = \frac{I}{2\pi\sigma^2} \exp\left(-\frac{d^2}{2\sigma^2}\right))$. The x-position and y-position of beam source are fixed in

space at 7.5 mm and 7.5 mm, whereas the z-position of beam source is 92.5 mm. The standard deviation of beam source was used and the laser spot area was set as 1 mm^2 .

Based on the previous measurement of thermal conductivity [Adv. Mater. 2024, 2406147], that of the sapphire and CASN/glass film was set as $35 \text{ W}\cdot\text{m}^{-1}\cdot\text{K}^{-1}$ and $1.6 \text{ W}\cdot\text{m}^{-1}\cdot\text{K}^{-1}$, respectively.

The surrounding air was held constant at 20°C . At the top and side surfaces, a convective heat flux boundary condition was used, which is driven by the temperature difference between the converter and the surrounding atmosphere: $q = h(T_{\text{ext}} - T)$. Here q is the inward heat power and h is the heat transfer film coefficient.

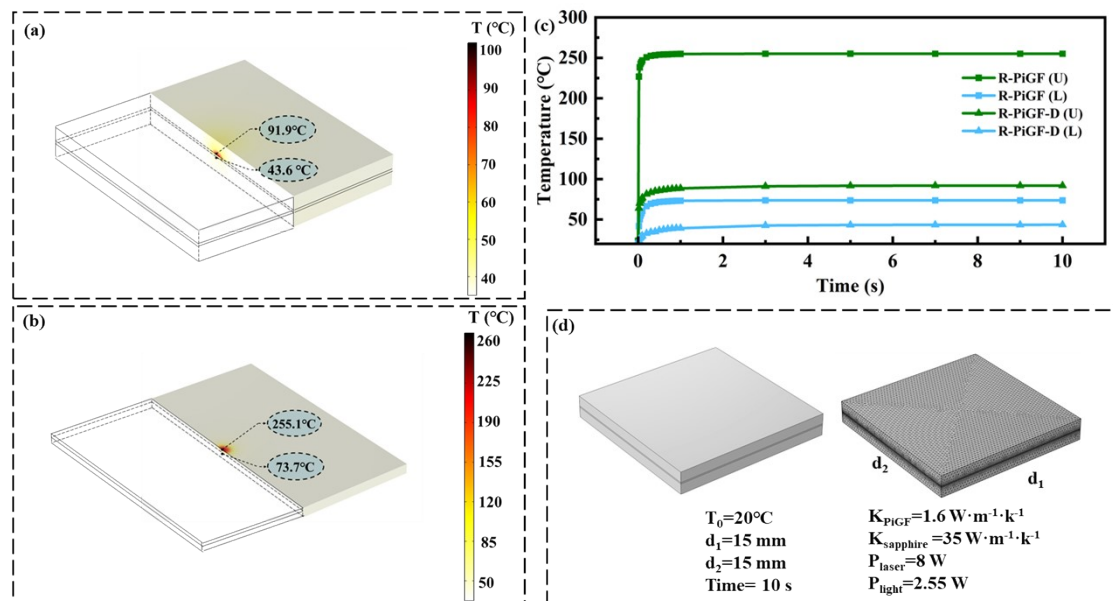


Figure S1 Simulated maximum upper and lower surface temperatures of (a) R-PiGF-D, (b) R-PiGF. (c) Two PiGF converters under various laser excitation times. (d) Thermal boundary conditions of R-PiGF-D converter.

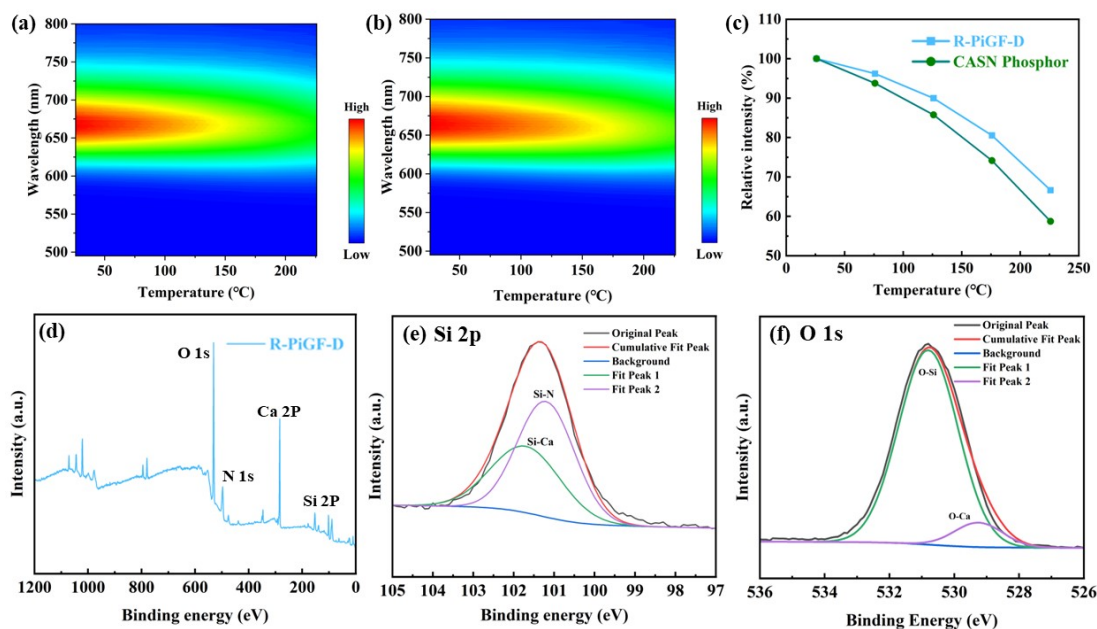


Figure S2 (a) Temperature dependent PL spectra of (a) CASN phosphor (b) CASN-PiGF. (c) Temperature-dependent relative integrated emission intensities of CASN-PiGF and CASN phosphor. Wide X-ray Photoelectron Spectroscopy (XPS) spectra of (d)R-PiGF-D and high resolutions XPS spectra of (e) Si 2p and (f) O 1s, respectively.

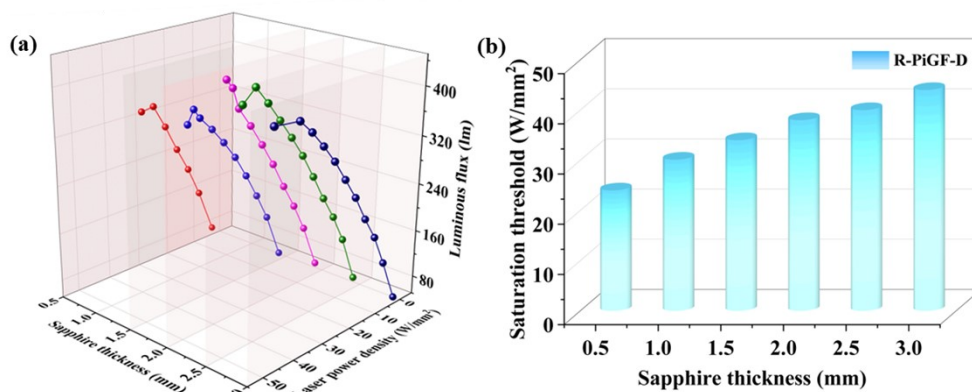


Figure S3 (a) Luminous fluxes and (b) saturation thresholds of R-PiGF-D converters with different sapphire thicknesses under various laser power densities.

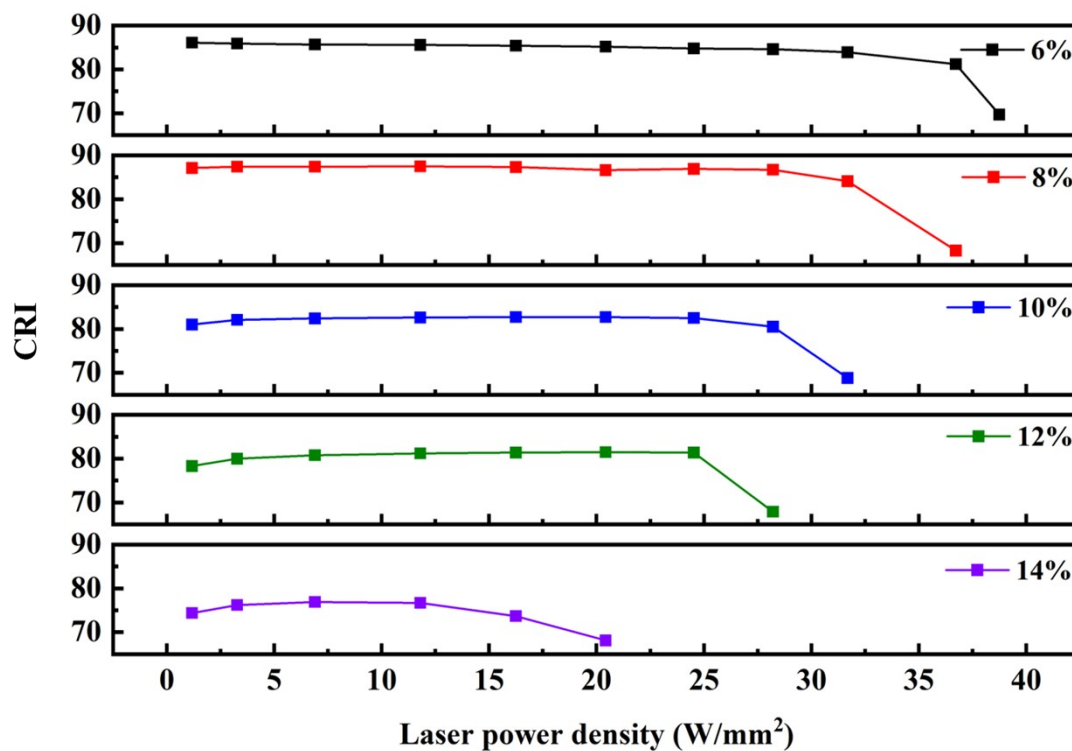


Figure S4 CRIs of Y/R-PiGF-Ds with different CASN concentrations under various laser power densities.